# Nonlinear Structure and Evolution of African Easterly Waves

Nathan R. Hardin

North Carolina State University, Raleigh, NC

## 1 Introduction

African easterly waves (AEWs) are important synoptic-scale weather systems affecting the tropical Atlantic and West Africa. During the boreal summer they propagate westward (Reed et al. 1977), modulating West African rainfall on a daily basis (Carlson 1969a, Carlson 1969b). Past studies have also shown AEWs to be responsible for the majority of tropical cyclone formation in the Atlantic Basin; 61% climatologically, but higher in individual seasons (e.g. Pasch and Avila 1994; Landsea et al. 1998).

Past studies (e.g., Rosenthal 1960, Merritt 1964, Burpee 1972) used a variety of observational platforms to better understand AEW formation and structure. Baroclinicity between equatorial Africa and the Sahara Desert results in the formation of the African Easterly Jet (AEJ). Contributions from baroclinic and barotropic growth mechanisms within the AEJ leads to the development of AEWs (Burpee 1972).

AEWs are characterized by a period ranging between three to five days, a wavelength of 2000 to 4000 km, and a maximum wave amplitude centered at 700 hPa (Carlson 1969a,Burpee 1972, Reed et al. 1988). Perturbations in the vorticity field range across 20° of latitude, with the center located near 20°N (Carlson 1969a, Reed et al. 1977).

Shapiro (1977) investigated the critical period during which a disturbance (AEW) transforms into a tropical depression. The main physical process involved in this transformation

pertains to the redistribution of eddy kinetic energy. This redistribution results in a more nonlinear, or vortical, structure of the AEW. Similar research was done by Estoque and Lin (1977), in which diabatic heating was converted into kinetic energy, and subsequently transferred down towards the surface in order to continue providing a fuel source for the AEW.

Cho et al. (1983) took a first order approximation of the vorticity equation, accounting only for vorticity generated by cumulus clouds, and applied it to the tropics. Their findings suggest the ability of cloud-scale vorticity to be generated and ingested into the large-scale environment by convection leads to higher AEW vorticity and development potential. Kwon and Mak (1990) studied the thermal structure of AEWs and tropical depressions, and stated that some heating threshold value must be overcome through convective latent heating in order for AEWs to undergo tropical cyclogenesis.

In other words, all of these studies lend support to the idea that AEWs undergoing tropical cyclogenesis exhibit nonlinear behavior. Whether through diabatic heating or vorticity generation, AEWs developing into tropical depressions were able to redistribute and enhance their system's kinetic energy. While the importance of nonlinearity is acknowledged, a deeper understanding is necessary in order to more fully understand its role in cyclogenesis of AEWs.

In the following presentation, composite structures based on measures of nonlinearity are shown. These composite structures are presented as evidence that AEW disturbances undergoing tropical cyclogenesis exhibit coherent vortex structures (CVS) rather than the classical, quasi-linear, Rossby wave (RW) solution. Measures of nonlinearity are computed and analyzed from a climatology AEW perspective. Finally, there is a brief summary of findings and ideas for future work.

# 2 Data and Methods

*a) Data*

Data used in this study is obtained from the European Centre for Medium-Range Weather Forecasts (ECMWF). The Re-analysis (ERA40) data set has a global resolution of 1.125 x 1.125 latitude-longitude, set on 22 vertical levels. The period of the study spans Une-October 1980-2001. Additionally, brightness temperature data from the CLOUD Archive User Service (CLAUS) is used for the time period June-October 1984-2001.

*b) Beta-Rossby Number Diagnostics*

Moore and Montgomery (2004) commented on the existence of diabatic Rossby vortexes (DRVs), whose features were characterized by closed circulations instead of alternating high/low, 'wave-like', structures. These DRVs were seen to be coherent structures reliant upon baroclinicity and diabatic heating for intensification, instead of large scale forcing (Moore and Montgomery 2005). Moore and Montgomery (2005) also hypothesized DRVs may be applicable as a growth mechanism in tropical processes, specifically the amplification and strengthening of AEWs into tropical cyclones.

Various studies in the past, not necessarily tropical in focus, have used a parameter referred to as the $\beta$-Rossby number to quantify the relationship between linear and non-linear vortex processes (Enagonio and Montgomery 2001, and references therein). When considering a vorticity maxima, the non-dimensional $\beta$-Rossby number is given by

$$R_\beta = V/L^2\beta$$

where V is the vortex/eddy's maximum tangential wind, L is the radius of maximum wind, and $\beta$ is the meridional gradient of planetary vorticity. Whether considering a vortex or an eddy, a large number corresponds to a localized coherent vortex with weak Rossby wave

dispersion. A small number conveys a weak feature, continually dissipating through Rossby wave dispersion (Enagonio and Montgomery 2001). Another way of viewing the $\beta$-Rossby parameter is as a comparison between the self-advection and planetary advection terms of the barotropic vorticity equation.

For the purposes of this study, the distinction between linearity and nonlinearity is based on the $\beta$-Rossby number of identified vorticity maximas. Linear vorticity maximas are those with $R < .4$, whereas nonlinear vorticity maximas are characterized by $R > 2$.

*c)Vorticity Maxima Identification*

An objective algorithm was developed for the feature based detection of coherent vortical structures (CS). The 700hPa surface of Ertel potential vorticity (PV) was examined to identify local PV maximas. If an area had a .2 PVU value higher than any point within 600 kilometers radius, with the ability to draw an enclosed .1 PVU contour, a local maximum was identified. The algorithm also estimates the radius of maximum wind (RMW) and associated tangential wind velocity. Tangential wind velocity and RMW are used to compute the Beta-Rossby number for each identified vorticity maxima. An example of the vorticity maxima identification map output is shown in Figure 1.

*d) Compositing Technique*

Structures were composited based on their $\beta$-Rossby Numbers. As mentioned earlier, vorticity maxima with $R_\beta < .4$ were grouped into the linear category, wherear maximas with $R_\beta > 2$ were deemed nonlinear. Using the 22 vertical levels for a variety of atmospheric variables (e.g., PV, Theta, Omega, Divergence, Relative Humidity), each group was composited to gain an idea of the 'average' structure. This was accomplished by creating a storm-relative composite, whereby all identified maximas were moved to a reference latitude and longitude.

Maximas from 0° to 30°N latitude, and 16°W to 100°W were included in the compositing process.

# 3 Results and Discussion

*a) Composite Structures*

Initial analysis of composite structures for both the linear and nonlinear cases were constructed using Ertel PV. Figures 2 and 3 show the resultant composite structure of PV and wind vectors. Fig. 2 shows the linear composites, while nonlinear composites are shown in Fig. 3. As can be seen in the linear case at 600hPa (Fig. 2), the wind vector field shows existence of a trough. This trough is analogous with the existence of an AEW. Apart from the 600mb surface, where closed contours of PV exist, the structure is more open wave-like than closed vortex-like. When comparing Fig. 3, or the nonlinear case, the comparative strength is clearly seen. Multiple closed PV contours exist at not just 600hPa, but from 500hPa down through 775hPa. While number of contours is not necessarily of importance, the clear separation of the AEW PV maxima compared to the background PV is. The nonlinear case composite structure is not just more intense with regards to the maxima itself, but it is also surrounded by a weaker PV environment. This fact further supports the idea that some AEWs are independent and coherent vortices instead of Rossby waves.

Figure 4 shows the brightness temperature composited with 600hPa PV. The nonlinear case is seen to be have colder brightness temperatures (i.e. stronger convection) than the linear composites. While this may be expected, it is additional evidence supporting the idea that nonlinear AEWs (as classified in this study) may be more apt to undergo tropical cyclogenesis due to a more favorable structure. Also of interest in Fig. 4 is how the intense convection seems to be better co-located with the PV maxima, whereas, in the linear case, the highest intensity convection is located slightly to the south and east of the PV maxima.

After horizontal cross sections were analyzed, vertical cross sections were constructed. Vertical cross sections were plotted with relative humidity, omega, and theta, as well as PV and theta. These cross sections are shown for the linear and nonlinear composites in Figure 5. The cross sections reveal the nonlinear composites have more abundant moisture, which extends deeper into the atmosphere than the linear cases. Juxtaposed with the deeper humidity is more robust upward motion (omega). At its most intense point, omega in the nonlinear case is nearly twice that found in the linear composite. When considering the PV composites shown in Fig. 5, the relative intensity of the nonlinear cases once again becomes apparent. While both the linear and nonlinear composites have a PV maximum centered near 600hPa, the nonlinear composite is comprised of a higher PVU maximum. Also, the nonlinear composite has a PV maxima which reaches a greater vertical extent, approximately 700hPa to 400hPa, than the linear case, which extends from roughly 600hPa to 500hPa. In the nonlinear composite, in the upper troposphere (250hPa-300hPa), there is evidence of stronger anticyclone development. In the nonlinear case at upper levels, above the vortex, the lower PV values indicate a stronger diabatic redistribution of PV (Fig. 5).

*b) $\beta$-Rossby Number Statistics*

AEW 'genesis' cases were tracked from their emergence off the African continent until the 6 hour period before undergoing tropical cyclogenesis. $\beta$-Rossby Number was recorded for each 6 hour interval using the AEW track locations. Genesis cases were recorded for each season from 1990 through 2001. Similarly, AEWs not resulting in tropical cyclogenesis (null cases) were tracked and recorded for the years 1992, 1993, and 1999. These years were selected due to their wide range of seasonal meridional wind and brightness variances. In all, there were 73 separate AEWs leading to tropical cyclones, while 27 null cases were tracked. The 73 genesis cases were comprised of 1125 separate time periods, whereas the null cases

comprised 530 times.

Using these periods, the average $\beta$-Rossby number for genesis and null cases was computed. In addition to the $\beta$-Rossby number, other statistical parameters (e.g. median and standard deviation) were computed for the cases. Table 1 shows the mean $\beta$-Rossby number values for the genesis and null cases. As can be seen, cases leading to tropical cyclones had an average value of greater than 2, whereas those not experiencing cyclogenesis averaged less than 2. These numbers support the claim that nonlinearity leads to a greater likelihood of AEWs experiencing genesis. Figure 6 shows a scatterplot of all time values from the genesis and null cases, as well as their respective linear regression lines. There is not much of a difference between the null and genesis wave cases until they progress past 60°W. At this longitude, using the regression line as an indicator, the genesis cases are, on average, stronger as they continue to move westward. Using Fig. 6, one may state that if an AEW maintains a higher $\beta$-Rossby number as it moves westward of 60W, it is more likely to experience cyclogenesis than an AEW whose Beta-Rossby number is lower at the same longitude. Even at the western edge of the Atlantic Basin, AEWs undergoing tropical cyclogenesis still had an average $\beta$-Rossby number near 2.

# 4 Summary and Future Work

Using a parameter known as the $\beta$-Rossby number as an indicator, the role of nonlinearity in AEW structure and evolution has been examined. Separating AEWs into classifications of 'linear' and 'nonlinear', composite structures of the waves were constructed.

- Linear wave composites suggest a classical, Rossby wave behavior, where perturbations exhibit wave-like propagation within the large-scale flow
- Nonlinear composites support that AEWs exhibit a coherent vortex structure, instead of being 'wave-like'

- A more robust convective signal and coupling to the PV maxima exists for nonlinear wave cases
- Cross sectional areas reveal deeper and more intense moisture in nonlinear cases, co-located with omega values double those found in the linear composites
- PV composites show nonlinear cases are deeper and more intense than the linear cases, while also showing signs of preconditioning and altering the ambient environment
- Preliminary statistics show cases undergoing tropical cyclogenesis have an average $\beta$-Rossby number greater than 2
- Wave cases not experiencing cyclogenesis had a mean $\beta$-Rossby number less than 2
- These findings support the idea that those AEWs exhibiting nonlinear structure and behavior are more apt to become tropical cyclones, especially if maintaining this structure west of 60°W (Fig.6).

In the future, individual case studies will be incorporated to gauge their $\beta$-Rossby behaviors. Preferably, a variety of AEW cases should be studied to ensure more robust statistical validity. Also, more null cases may be included to accomplish a greater sample size when computing $\beta$-Rossby number statistics.

## *Acknowledgments*

Dr. Anantha Aiyyer supervised this study. Funding was provided by North Carolina State University Start-Up Funds. ECMWF ERA40 data can be obtained through the ECMWF server, available at ($http://www.ecmwf.int/$). CLAUS brightness data is available through the British Atmospheric Data Centre, found at
($http://www.badc.nerc.ac.uk/cgi-bin/data_browser/badc/claus/$).

# References


Burpee, R. W., 1972: The origin and structure of easterly waves in the lower troposphere of North Africa. *J. Atmos. Sci.*, **29,** 716–726.

Carlson, T. N., 1969a: Some remarks on African disturbances and their progress over the tropical Atlantic. *Mon. Wea. Rev.*, **97,** 716–726.

Carlson, T. N., 1969b: Synoptic histories of three African disturbances that developed into Atlantic hurricanes. *Mon. Wea. Rev.*, **97,** 256–276.

Cho, H. R., M. A. Jenkins, and J. Boyd, 1983: A first order vorticity equation for tropical easterly waves. *J. Atmos. Sci.*, **40,** 958–968.

Enagonio, J., and M. T. Montgomery, 2001: Tropical cyclogensis via convectively forced vortex rossby waves in a shallow water primitive equation model. *J. Atmos. Sci.*, **58,** 685–705.

Estoque, M. A., and M. S. Lin, 1977: Energetics of easterly waves. *Mon. Wea. Rev.*, **105,** 582–589.

Kwon, H. J., and M. Mak, 1990: A study of the structural transformation of the African easterly waves. *J. Atmos. Sci.*, **47,** 277–292.

Landsea, C. W., G. D. Bell, W. M. Gray, and S. B. Goldenberg, 1998: The extremely active 1995 Atlantic hurricane season: Environmental conditions and verification of seasonal forecasts. *Mon. Wea. Rev.*, **126,** 1174–1193.

Merritt, E. S., 1964: Easterly waves and perturbations, a reappraisal. *J. Appl. Meteor.*, **3,** 367–382.

Moore, R. W., and Michael T. Montgomery, 2004: Reexamining the Dynamics of Short-Scale, Diabatic Rossby Waves and Their Role in Midlatitude Moist Cyclogenesis. *J. Atmos. Sci.*, **61,** 754–768.

Moore, R. W., and Michael T. Montgomery, 2005: Analysis of an Idealized, Three-Dimensional Diabatic Rossby Vortex: A Coherent Structure of the Moist Baroclinic Atmosphere. *J. Atmos. Sci.*, **62,** 2703–2725.

Pasch, R., and L. A. Avila, 1994: Atlantic tropical systems of 1992. *Mon. Wea. Rev.*, **122,** 539–548.

Reed, R. J., Donald C. Norquist, and Ernest E. Recker, 1977: The structure and properties of african wave disturbances as observed during phase III of GATE. *Mon. Wea. Rev.*, **105,** 317–333.

Reed, R. J., A. J. Simmons, M.D. Albright, and P. Unden, 1988: The role of latent heat release in explosive cyclogenesis: Three examples based on ECMWF operational forecasts. *Wea. Forecasting*, **3,** 217–229.

Rosenthal, S. L., 1960: A simplified linear theory of equatorial easterly waves. *J. Meteor.*, **17,** 484–488.

Shapiro, L. J., 1977: Tropical storm formation from easterly waves: A criterion for development. *J. Atmos. Sci.*, **34,** 1007–1021.

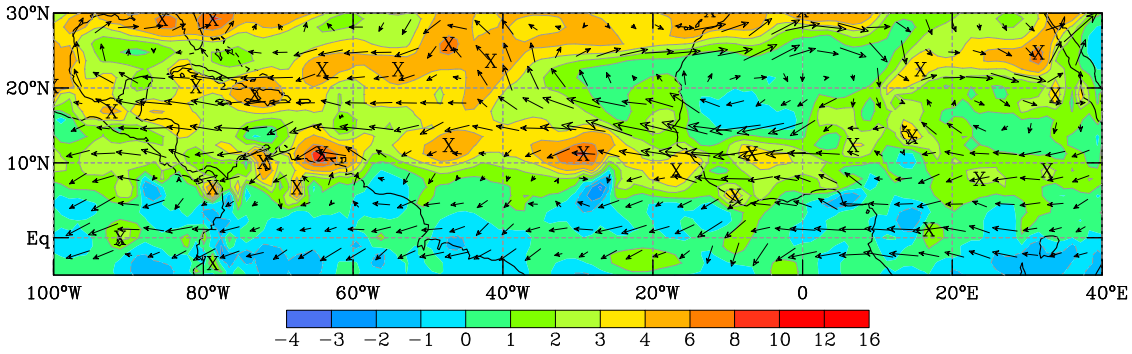


Figure 1: Example of vorticity maxima tracking algorithm for 09/07/99 at 06z: 600hPa Ertel PV in .1 PVU($10^{-7}$ K$kg^{-1}m^2s^{-1}$, shaded) and vector winds. The position of each objectively identified coherent structure is denoted by 'x'.

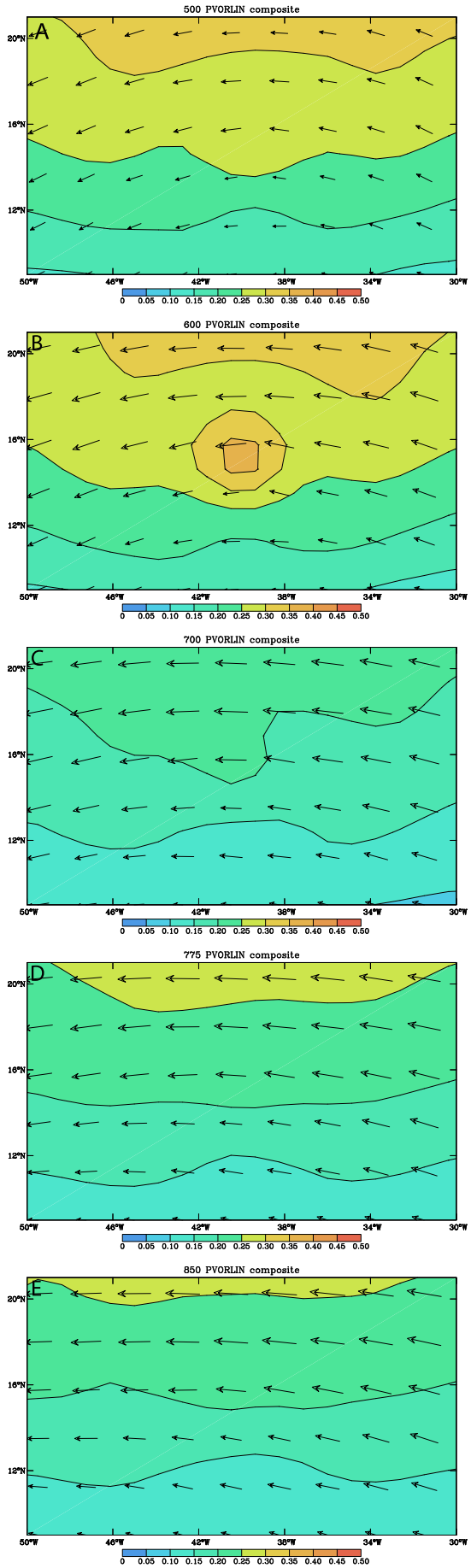


Figure 2: Linear PV composite in PVU ($10^{-6}$ K$kg^{-1}m^2s^{-1}$) for (a)500hPa; (b)600hPa; (c)700hPa; (d)775hPa; (e)850hPa

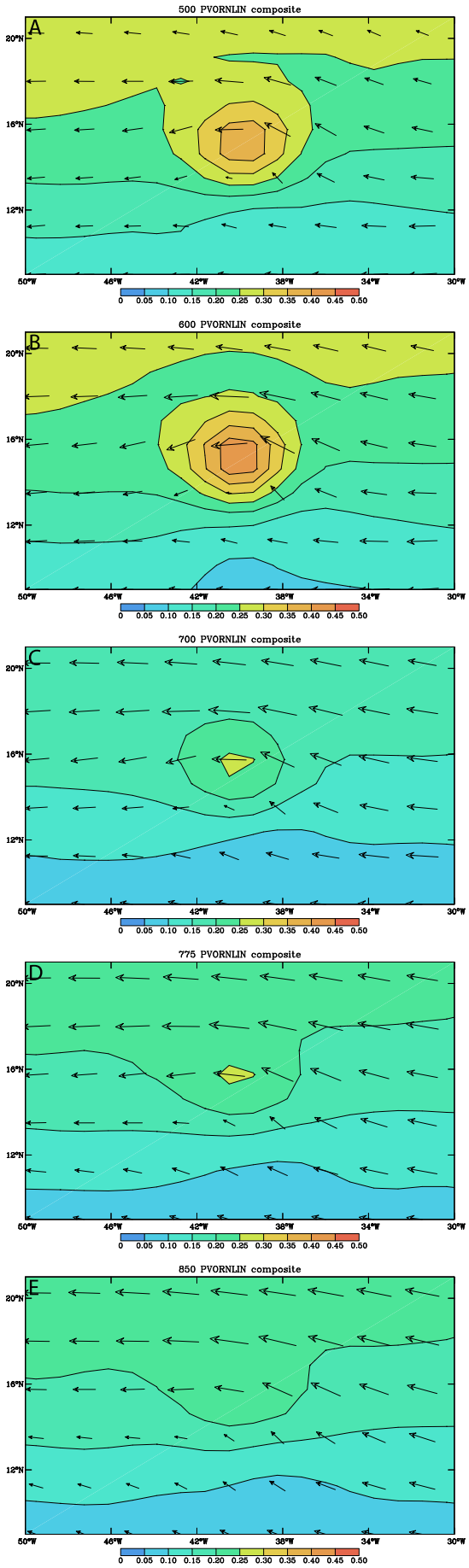


Figure 3: As in Fig.2, but for Nonlinear case

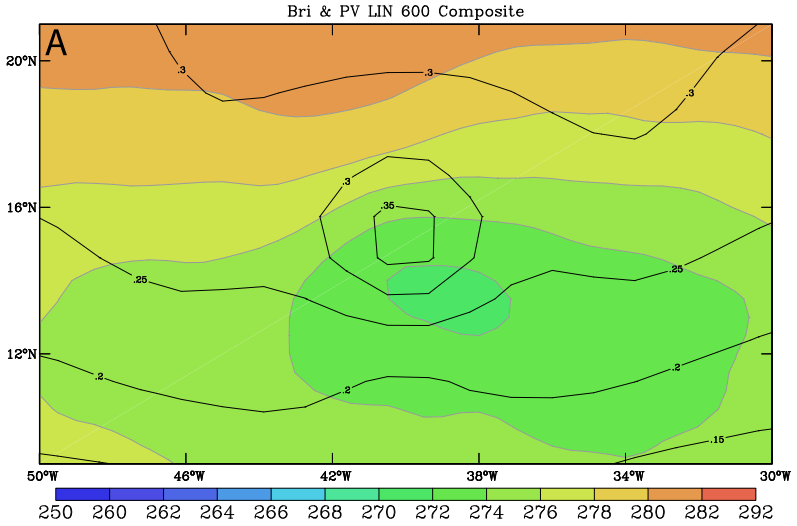


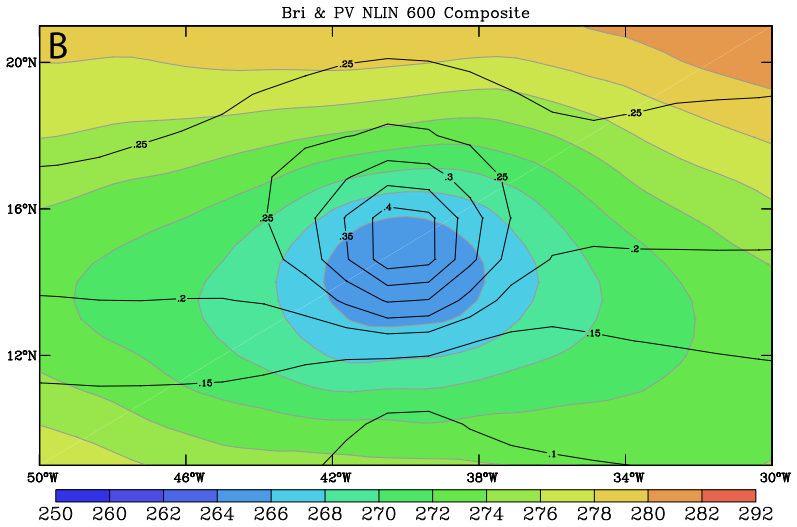


Figure 4: Brightness Temperature(K) (shaded) and 600hPa PV composite (PVU) for (a)linear and (b)nonlinear cases

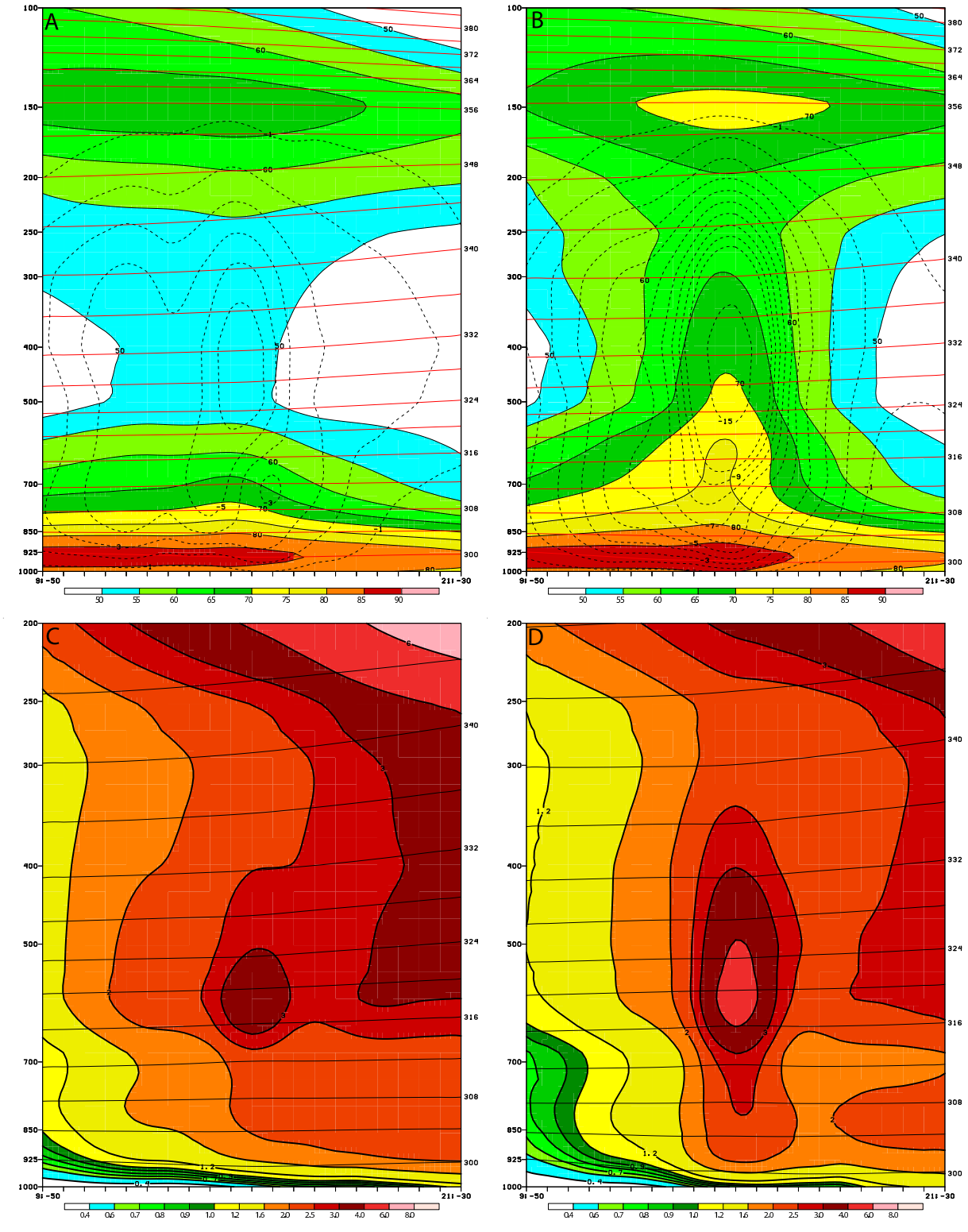


Figure 5: Composite cross sections of relative humidity in percent (shaded) and vertical velocity omega in (m/s) (contoured) for (a)linear and (b)nonlinear; and PV in PVU for (c)linear and (d)nonlinear cases

Table 1: Mean Beta-Rossby number values for genesis and null cases

| Source | Mean |
|---|---|
| Genesis Cases | 2.24 |
| Null Cases | 1.85 |

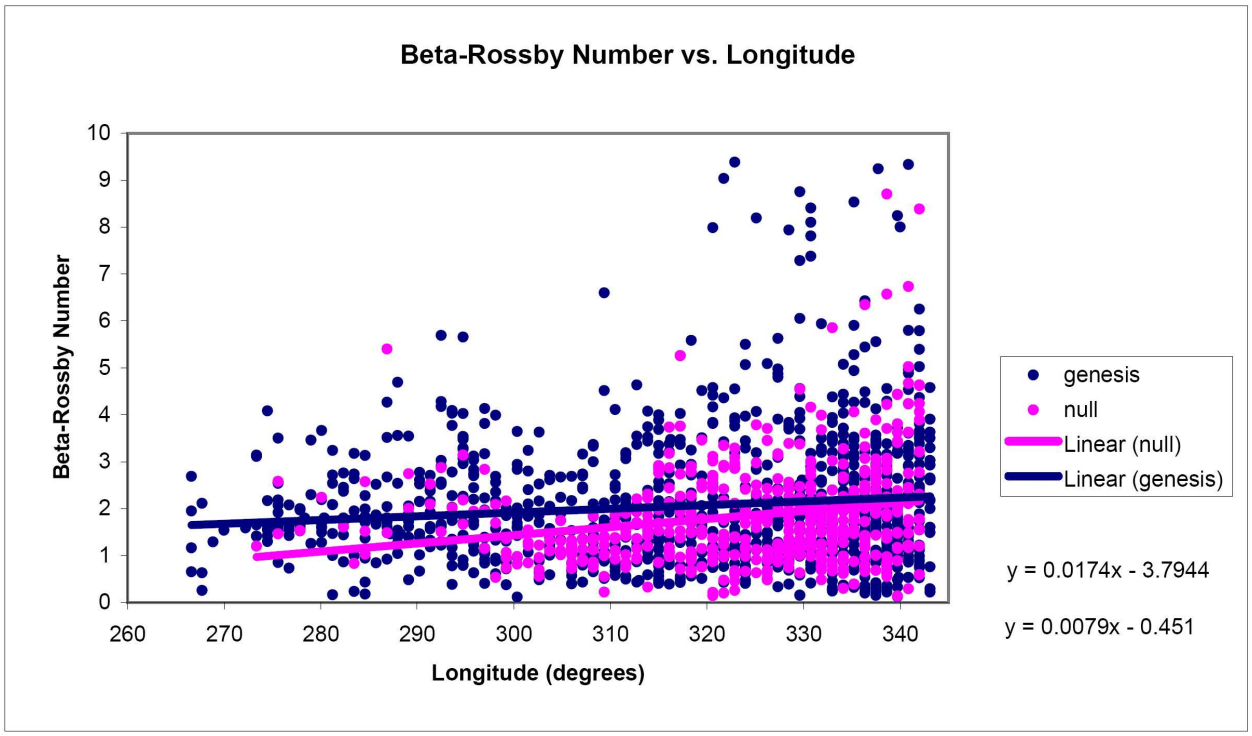


Figure 6: Scatterplot and regression lines of Beta-Rossby number versus longitude for genesis and null cases